

# HEAT TREATMENT OF COBALT-BASE ALLOY SURGICAL IMPLANTS WITH HYDROXYAPATITE-BIOGLASS FOR SURFACE BIOACTIVATION

H. Minouei\*, M. H. Fathi, M. Meratin and H. Ghazvinizadeh

\* h\_minouie@yahoo.com

Received: January 2012

Accepted: August 2012

Department of Materials Engineering, Isfahan University of Technology, Isfahan, Iran.

**Abstract:** ASTM F-75 Cobalt-base alloy castings are widely used for manufacturing orthopedic implants. The alloy needs both homogenization and solutionizing heat treatment after casting, as well as bioactivation of the surface to increase the ability of tissue bonding. In this study, ASTM F-75 Cobalt-base substrate was heat treated at 1220°C for 1 hour in contact with Hydroxyapatite-Bioglass powder in order to solutionize and homogenize the microstructure and promote surface bioactivation. In order to bioactivity evaluation, heat treated specimens were immersed in Simulated Body Fluid (SBF). Surface of specimens before and after the immersion was analyzed by Scanning Electron Microscopy (SEM), Energy Dispersive Spectroscopy (EDX) and X-Ray Diffraction (XRD). Results showed an appropriate microstructure with bioactive layer on the surface of specimens after heat treatment. In vitro evaluation results and formation of bone-like apatite layer on specimens indicated that heat treated samples were potentially suitable for medical orthopedic applications under highly loaded conditions.

**Key words:** Bioactive coating, Bioglass, Cobalt-base alloy, Hydroxyapatite, Solutionizing

## 1. INTRODUCTION

Metallic biomaterials consist of stainless steel, Cobalt-base alloys, and titanium alloys are widely used for manufacturing of orthopedic prosthesis due to their biocompatibility, good mechanical properties and excellent corrosion resistance. Co-Cr and Co-Cr-Mo alloys are the safest materials used in hip and knee prosthesis development. However, these materials are classified as bioinert materials, because they can not bond to living bone [1, 2].

On the other hand, some of the biomaterials such as, Hydroxyapatite (HA) and Bioactive Glass (BG) are bioactive [3]. This means that when they are placed in contact with human blood plasma, they promote osteointegration and they will be chemically bond to bone. However, these bioceramics can not be used in highly loaded conditions due to their low mechanical properties. One of the best method for obtaining implants with both good mechanical properties and bioactive surfaces is applying HA or BG coating on metallic implants surfaces [4, 5]. For this purpose, several coating technique such as plasma spray [6], electrophoretic deposition [7], sol- gel [8 and 9], biomimetic process [10] and thermal spraying [11] have been developed.

The most common process for manufacturing of

Cobalt-base ASTM F-75 alloy orthopedic and dental implants is investment casting [12]. The main strengthening mechanism in the as-cast conditions is carbide precipitation, but it also causes low ductility observed under such conditions. An alternative method to enhance ductility and other mechanical properties such as yield and ultimate tensile strengths is solution treatment. This heat treatment carries out at temperatures around 1220 °C for about 1 hr to obtain homogeneous carbide distribution in Cobalt matrix [13, 14, 15 and 16]. So, performing this process on ASTM F-75 alloy with simultaneous surface bioactivation is very interesting, because of shortening the manufacturing process, savings in time and energy [17]. In this work, the surface bioactivation of Cobalt-base ASTM F-75 alloy during solution heat treatment was investigated. Bioactivity of the specimens was also evaluated by In vitro via immersion in Simulated Body Fluid (SBF) and investigation the bone-like apatite layer formation.

## 2. EXPERIMENTAL PROCEDURE

### 2. 1. Specimens preparation

ASTM F-75 Cobalt-base alloy was melted in an induction furnace and was casted into

investment casting molds, which were designed in order to obtain 6 specimens with dimensions of  $12 \times 12 \times 4$  mm. The molds were fabricated using phosphate bonded investment. Molten metals were poured at  $1450^\circ\text{C}$  into investment molds which were preheated at  $950^\circ\text{C}$ . Table 1 shows standard chemical composition of ASTM F-75 alloy used as a substrate. Then, specimens were grounded with silicon carbide papers ranging from 80 to 2400 grit and polished using 30 microns alumina paste. After polishing, specimens were gently washed in ethanol and dried. After preparation, surface roughness of the specimen was measured and the average number of  $0.03\text{ }\mu\text{m}$  was obtained.

Bioglass with a close composition to Bioglass® 45S (45wt%  $\text{SiO}_2$ , 49wt%  $\text{CaO}$  and 6wt%  $\text{P}_2\text{O}_5$ ) was prepared by sol-gel method. BG agglomerates with average size of

$10\text{ }\mu\text{m}$  which consist of particles with average size of  $80\text{ nm}$  and also hydroxyapatite powder (Merck with average particle size of  $10\text{ }\mu\text{m}$ ) were used in this study. Mixture of HA-BG, contained 70wt% of HA was placed between polished metallic surface specimens. A uniaxial pressure of 65 MPa was applied to non polished surfaces using a fixture as shown in Figure 1. Metallic specimens under pressure of 65 MPa were heat treated in contact with HA-BG mixture in  $1220^\circ\text{C}$  for 1 hour followed by water quench. In order to prevent the decarburization and unwanted chemical reaction between atmospheres and the alloy, the specimens were maintained in stainless steel foil and sealed by

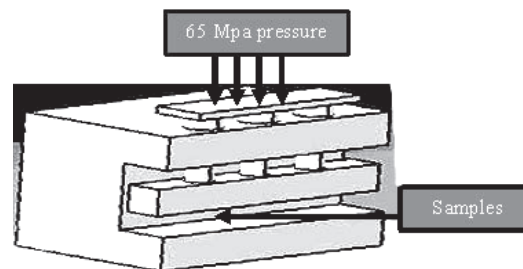


Fig. 1. Fixture used to apply 65MPa uniaxial pressure.

fireclay. After heat treatment, specimens were washed with deionized water and dried.

## 2. 2. In vitro Evaluation

For in vitro evaluation, simulated body fluid was prepared with ionic concentration of nearly equal to human blood plasma according to Kokubo instructions (Table2) [18]. After heat treatment Specimens were immersed in simulated body fluid and were hold in a water bath at  $37^\circ\text{C}$  for 4 week.

Volume of the SBF needed for immersion of specimens was calculated according to following equation;

$$V_s = S_a / 10 \quad (1)$$

Table 2. Nominal ion concentrations of SBF in comparison with those in human blood plasma.

| Ion                 | Ion concentrations (mM) |       |
|---------------------|-------------------------|-------|
|                     | Blood plasma            | SBF   |
| $\text{Na}^+$       | 142.0                   | 142.0 |
| $\text{K}^+$        | 5.0                     | 5.0   |
| $\text{Mg}^{2+}$    | 1.5                     | 1.5   |
| $\text{Ca}^{2+}$    | 2.5                     | 2.5   |
| $\text{Cl}^-$       | 103.0                   | 147.8 |
| $\text{HCO}_3^-$    | 27.0                    | 4.2   |
| $\text{HPO}_4^{2-}$ | 1.0                     | 1.0   |
| $\text{SO}_4^{2-}$  | 0.5                     | 0.5   |
| pH                  | 7.2-7.4                 | 7.4   |

Table 1. Standard chemical composition of Co-base ASTM F-75 alloy.

| Element | ASTM F-75 |
|---------|-----------|
| Co      | Balance   |
| Cr      | 27-30     |
| Mo      | 5-7       |
| Si      | 1.0       |
| Mn      | 1.0       |
| Ni      | 1.0       |
| Fe      | 0.75      |
| C       | 0.35      |

Where:

$V_s$ : volume of SBF (ml)

$S_a$  = apparent surface of specimens ( $\text{mm}^2$ )

Specimens were immersed in SBF for 1, 2, 3 and 4 week at 37 °C. After each predicted period of time, specimens were washed with deionized water, dried and stored.

### 2. 3. Characterization Methods

X-Ray Diffraction (XRD) technique (Philips X'Pert-MPD system with a Cu K $\alpha$  wavelength of 1.5418 Å) was used to analyze and study the phase structure present in the raw materials and the surface of specimens after heat treatment. The diffractometer was operated at 40 kV and 30 mA at a step size of 0.05.

Scanning Electron Microscopy (SEM) (Phillips XL 30) was used to study the surface of specimens after heat treatment.

ASTM F-75 alloy substrate microstructure was studied by optical microscopy. After preparation, the specimens electrolytically were etched in 95% H<sub>2</sub>O and 5% HCl for 1 second using voltage 5V. Photomicrographs were quantitatively analyzed by Image Tool software.

## 3. RESULTS AND DISCUSSION

### 3. 1. Microstructure and Phase Study of Bioactive Layer and Substrate

Figure 2(a) shows the as-cast microstructure of ASTM F-75 alloy and Figure 2(b) shows the microstructure of the alloy after solution treatment. Solution treatment causes homogeneous carbides distribution as shown in Figure 2(b). Figure 2(b) shows that solutionizing heat treatment gave rise to preferential carbide dissolution. The carbides precipitation relatively became finer with homogeneous distributions and also a large number of it was confined to the grain boundaries. It seems that solution heat treating of alloys promotes preferential grain boundary precipitation and carbide coarsening [14]. Figure 3 shows the XRD pattern of as-cast ASTM F-75, demonstrated the presence of M<sub>23</sub>C<sub>6</sub> carbide in face center cubic (FCC) Cobalt matrix.



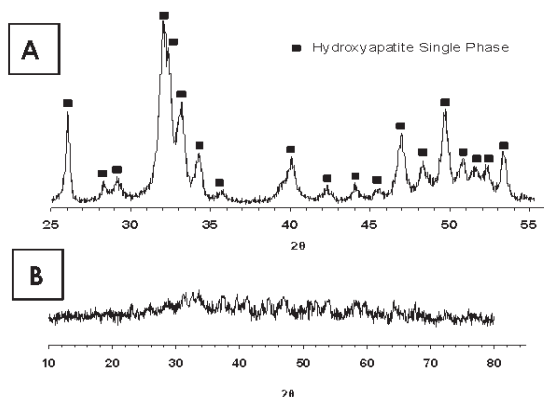
Fig. 2. Microstructure of ASTM F-75 alloy in, (A) as- cast condition and (B) after solution treatment.



Fig. 3. X-ray diffraction pattern of as-cast Co-Cr-Mo alloy.

XRD patterns of HA and BG used for preparing bioceramic mixture are shown in Figures 4(a) and 4(b), respectively. According to these results, HA has a single phase structure and BG has an amorphous (non crystalline) structure.

XRD pattern of the surface of specimen after heat treatment (Figure 5) demonstrates the presence of tricalcium phosphate- $\beta$  ( $\beta$ -TCP), wollastonite, Cr<sub>2</sub>O<sub>3</sub> and hydroxyapatite on the surface. Commercial HA transforms to other calcium phosphate such as  $\beta$ -TCP at temperature higher than 900 °C. Presence of  $\beta$ -TCP probably occurred due to the partial transformation of HA during the heat treatment. Presence of this more



**Fig. 4.** X-ray diffraction patterns of bioactive biomaterials, (A) hydroxyapatite, and (B) bioglass.

soluble phase in bioactive layer increases the releasing Ca and  $\text{PO}_4$  ions in surrounding tissue.

Wollastonite phase may be formed during the heat treatment because non-crystalline structure was transformed to ceramic and formed a glass-ceramic in elevated temperatures. Even though it was tried to minimize substrate reaction to atmosphere, small amount of  $\text{Cr}_2\text{O}_3$  was formed on the surfaces. According to XRD patterns, during the heat treatment, excessive surface oxidation may occur due to the product of decomposition reaction as HA transforms to  $\beta$ -TCP, which leads to formation of  $\text{H}_2\text{O}$ . This causes trapping of ceramic agglomerates on the surface and helps to the mechanical bonding of

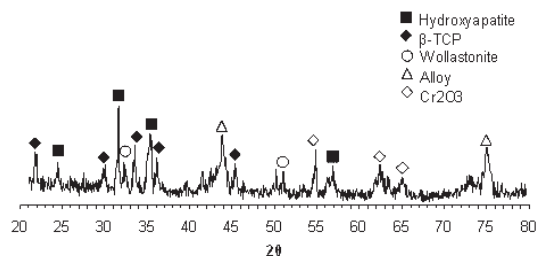


**Fig. 5.** X-ray diffraction pattern of specimen after heat treatment.

bioactive layer to substrate.

Figure 6(a) and (b) shows a bioactive coating on Co-Cr-Mo substrate. A continuous and homogenous bioactive layer on the surface of specimens can be clearly observed. This is probably due to the melting of the bioactive glass, because melting point of bioglass is close to the common solution treatment temperature used in this work. This assumption becomes more approved when attention to uniaxial pressure equal to 65MPa applied to specimens. Furthermore, this pressure encourages bioglass melting according to the Clausius-Clapeyron equation. In the other words, bioglass acting as a binder among HA particles in mixture leads to ceramic powder bonding beside, it has bioactive properties which promote osteointegration.

Cross section micrograph demonstrated the

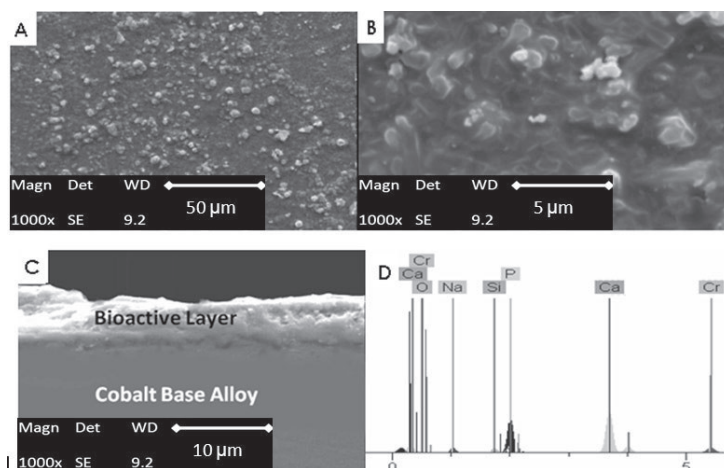


**Fig. 6.** SEM micrograph of the specimen surface after heat treatment, (A), (B) in different magnification, (C) cross section and (D) EDX elemental spectrum of surface.



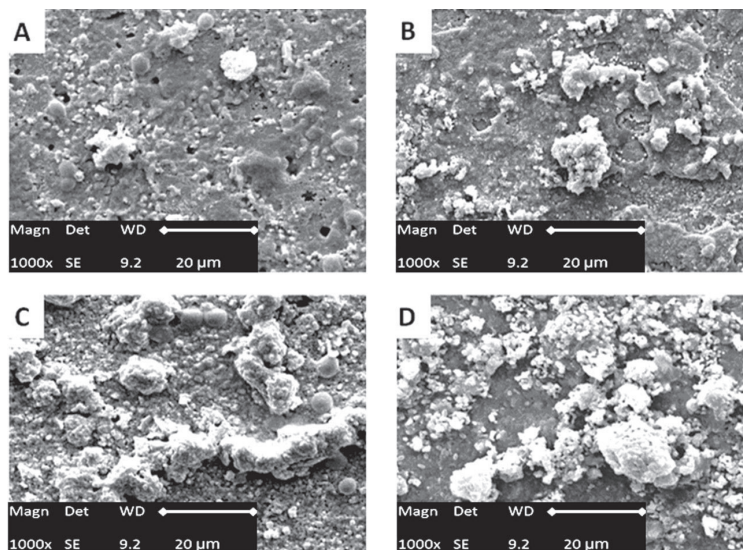


**Fig. 7.** SEM micrograph of specimen's surface after immersion in SBF for, (A) 1 week, (B) 2 week, (C) 3 week and (D) 4 week.

thickness of coating range from 6 to 10μm as shown in Figure 6(c). The EDX elemental spectrum shows the presence of Ca and P from HA and BG, Na and Si from BG and Cr from substrate (Figure 6(d)). Whereas Ortiz et al reported only the presence of ceramic agglomerate on the oxidized surface of substrates and they did not observed any sintering phenomena among the bioceramic powder [15]. These differences between results which were reported by Ortiz et al and the results of the present investigation may be depends on the type of bioglass and governing condition in heat treatment such as preventing oxidation, manner type of applying the pressure and powder fixing quality between metallic surfaces.

### 3. 2. In vitro Bioactivity Evaluation

Figure 7 shows the SEM micrographs of specimens after immersion in SBF. These micrographs demonstrate the nucleation and growth of bon-like apatite layer with increasing the immersion time, which confirms surface bioactivation. The size and number of apatite precipitation increased with the immersion time as well as thickness of them.

By quantitative image analysis of these micrographs, an increase in the percentage of

apatite formation on the surface was specified (Figure 8). After one week immersion in SBF, 6.5% of surface was covered with apatite precipitation which increasingly reaches to 61.1% after 4 weeks immersion in SBF.

Figure 9 shows pH variation with immersion time. The pH value in SBF increased during the first 3 days after immersion, and then it slightly decreased until it reached to 7.36 after 4 weeks. An increase in pH may occur due to ionic exchange between  $\text{Ca}^{2+}$  ions from bioactive layer and  $\text{H}^{+}$  ions from SBF and it is mostly because presence of

BG in bioactive layer. A Decrease in pH value determines that apatite precipitation starts after 3 days. In addition to apatite has relatively alkaline

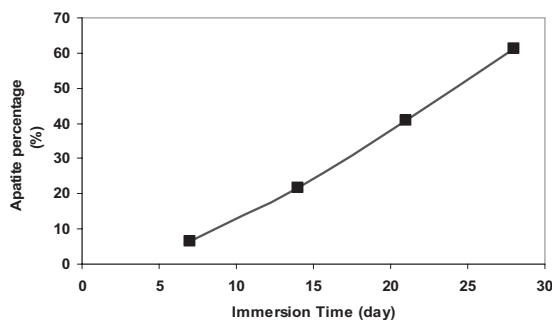


**Fig. 8.** Variation of apatite formation on surface with immersion time.



**Fig. 9.** The changes of pH in SBF vs. time which illustrates an increase in pH during the first 3 days and a slight decrease because of apatite precipitation

effect on the pH of the medium. The pH value depends on the solubility or resorbability of the hydroxyapatite, in the way that the pH decreases as the solubility increases.

Promote bioactivation during the solutionizing heat treatment which is necessary for ASTM F-75 alloy after investment casting, is a very economical method that will reduce energy consumption, costs, and manufacturing time of final products. This technique will be beneficial for manufacturing dental and orthopedic implants with bioactive surfaces.

#### 4. CONCLUSION

Bioactive coating on Cobalt-base ASTM F-75 alloy can be obtained simultaneously with solution heat treatment. Results showed a profitable bioactive layer on the surface of specimens as well as an appropriate microstructure of substrate after heat treatment. In vitro, surface bioactivity evaluation showed apatite nucleation and growth on the surface of specimens indicates surface bioactivity improvement. Promote surface bioactivation during the solutionizing heat treatment could be an economical method for reduction of costs.

#### REFERENCES

1. Kohn, D. H., "Metals in medical applications. Current Opinion in Solid State Materials Science", 1998, 3, 309-316.
2. Hosseini, Sh., Arabi, H., Tamizifar, M., Zeyaei A. A., "Effects of Tensile Strength on Fatigue Behavior and Notch Sensitivity of Ti-6Al-4V." *Iranian Journal of Materials Science and Engineering*, 2006, 3(1), 9-15
3. Fathi, M. H., Hanifi, A., Mortazavi, V., "Preparation and bioactivity evaluation of bone-like hydroxyapatite nanopowder." *J MATER PROCESS TECH*, 2008, 202, 536-542.
4. Hench, L. L., Wilson, J., "An Introduction to Bioceramic." *World Scientific*, Singapore, 1993, 75-85.
5. Saremi, M., Motaghi Golshan, B., "Electrodeposition of Nano Size Hydroxyapatite Coating on Ti Alloy." *Iranian Journal of Materials Science and Engineering*, 2006, 3(3), 1-5
6. Ozyegin, L. S., Oktar, F. N., Goller, G., Kayali, E. S., Yazici, T., "Plasma-sprayed bovine hydroxyapatite coatings." *MATER LETT*, 2004, 58, 2605-2609
7. Wang, C., Ma, J., Cheng, W., Zhang, R., "Thick Hydroxyapatite Coatings by Electrophoretic Deposition." *Mater Lett*, 2002, 57, 99-105.
8. Fathi, M. H., Doostmohammadi, A., 2008, "Bioactive glass nanopowder and bioglass coating for biocompatibility improvement of metallic implant. *J MATER PROCESS TECH* doi:10.1016/j.jmatprotec.2008.03.051.
9. Gallardo, J., Galliano, P., "Bioactive and Protective Sol-Gel Coatings on Metals for Orthopaedic Prostheses." *J SOL-GEL SCI TECHN*, 2001, 21, 65-74.
10. Cortes, D. A., Medina, A., Escobedo, S., Lopez M. A., "Biomimetic Apatite Formation On A

- CoCrMo Alloy By Using Wollastonite, Bioactive Glass or Hydroxyapatite.” *J MATER SCI*, 2005, 40, 3509 – 3515.
11. Lia, H., Khora, K. A., Cheang, P., “Thermal Sprayed Hydroxyapatite Splats: Nanostructures, Pore Formation Mechanisms and TEM Characterization.” *Biomaterials*, 2004, 25, 3463–3471.
  12. Gomez, M., Mancha, H., Salinas, A., Rodríguez, J. L., Escobedo, J., Castro, M., Mendez, M., “Relationship between Microstructure and Ductility of Investment Cast ASTM F-75 Implant Alloy.” *J BIOMED MATER RES*, 1997, 34, 157–163.
  13. Herrera, M., Espinoza, A., Mendez, J., Castro, M., Lopez, J., Rendon, J., “Effect of C Content on the Mechanical Properties of Solution Treated As-Cast ASTM F-75 Alloys.” *J MATER SCI-MATER M*, 2005, 16, 607– 611.
  14. Cohen, J., Rose, R. M. J., “Recommended heat treatment and alloy additions for cast Co–Cr surgical implants.” *J Biomed Mater Res*, 1978, 12, 935–937.
  15. Dobbs, H. S., Robertson, J. L. M., “Heat Treatment of cast Co–Cr–Mo, for orthopedic implant use.” *J Biomed Mater Res*, 1983, 18, 391– 401.
  16. Montero-Ocampo, C., Talavera, M., Lopez, H., “Effect of Alloy Preheating on The Mechanical Properties of As-Cast Co-Cr-Mo-C Alloys. *Metall Mater Trans A*,” 1999, 30a, 611-620.
  17. Ortiz, J. C., Cortés, D., Escobedo, J., Almanza, J., “A heat treatment method for obtaining a bioactive Cobalt-base alloy.” *MAter Lett*, 2008, 62, 1270-1274.
  18. Kokubo, T., Takadama, H., “How Useful is SBF in Predicting in Vivo Bone Bioactivity?”, *Biomaterials*, 2005, 26, 4747–4756.